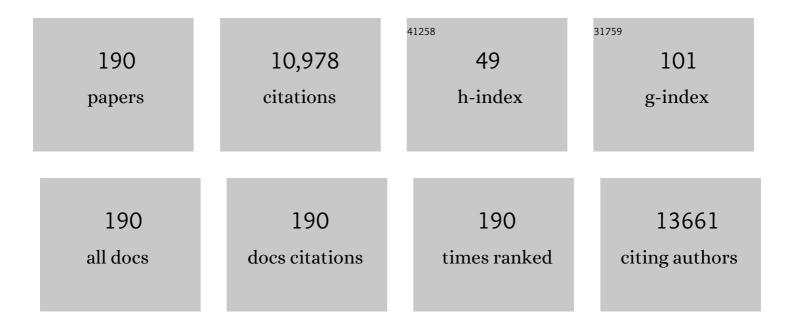
Zhi-Bo Liu

List of Publications by Year in descending order

Source: https://exaly.com/author-pdf/2017048/publications.pdf Version: 2024-02-01



<u>7ньВо Ци</u>

#	Article	IF	CITATIONS
1	Temperature-tunable optical properties and carrier relaxation of CuInP ₂ S ₆ crystals under ferroelectric-paraelectric phase transition. Journal of Materials Chemistry C, 2022, 10, 696-706.	2.7	9
2	Anisotropic Goos–Hächen shift in few-layer two-dimensional materials. Applied Physics Letters, 2022, 120, .	1.5	1
3	Stable Nanopores in Two-Dimensional Materials for Ion Conductivity Devices and Biosensors. ACS Applied Nano Materials, 2022, 5, 3611-3618.	2.4	3
4	Ultrafast Photocarrier Dynamics and Nonlinear Optical Absorption of a Layered Quaternary AgInP ₂ S ₆ Crystal. Journal of Physical Chemistry C, 2022, 126, 6837-6846.	1.5	5
5	Fabrication of Largeâ€Area Uniform Nanometerâ€Thick Functional Layers and Their Stacks for Flexible Quantum Dot Lightâ€Emitting Diodes. Small Methods, 2022, 6, e2101030.	4.6	3
6	Tuning the Thermal Transport of Hexagonal Boron Nitride/Reduced Graphene Oxide Heterostructures. ACS Applied Materials & Interfaces, 2022, 14, 22626-22633.	4.0	4
7	Recycling spent LiNi _{1-x-y} Mn _x Co _y O ₂ cathodes to bifunctional NiMnCo catalysts for zinc-air batteries. Proceedings of the National Academy of Sciences of the United States of America, 2022, 119, e2202202119.	3.3	89
8	Engineering Graphene Grain Boundaries for Plasmonic Multi-Excitation and Hotspots. ACS Nano, 2022, 16, 9041-9048.	7.3	7
9	A sliver deposition signal-enhanced optical biomolecular detection device based on reduced graphene oxide. Talanta, 2022, 249, 123691.	2.9	2
10	Stacking of 2D Materials. Advanced Functional Materials, 2021, 31, 2007810.	7.8	123
11	Laser-assisted two dimensional material electronic and optoelectronic devices. Journal of Materials Chemistry C, 2021, 9, 2599-2619.	2.7	18
12	Layer contribution to optical signals of van der Waals heterostructures. Nanoscale Advances, 2021, 3, 3114-3123.	2.2	0
13	Critical Strain-Induced Photoresponse in Folded Graphene Superlattices. ACS Applied Materials & Interfaces, 2021, 13, 21573-21581.	4.0	5
14	Tunable Optical Rotation in Twisted Black Phosphorus. Journal of Physical Chemistry Letters, 2021, 12, 4755-4761.	2.1	7
15	Magnetic Doping Induced Superconductivity-to-Incommensurate Density Waves Transition in a 2D Ultrathin Cr-Doped Mo ₂ C Crystal. ACS Nano, 2021, 15, 14938-14946.	7.3	7
16	Controllable graphene/black phosphorus van der Waals heterostructure tunneling device. Materials Letters, 2021, 300, 130189.	1.3	1
17	Thickness-dependent ultrafast charge-carrier dynamics and coherent acoustic phonon oscillations in mechanically exfoliated PdSe ₂ flakes. Physical Chemistry Chemical Physics, 2021, 23, 20666-20674.	1.3	7
18	Photothermalâ€Transport Imaging and Thermal Management of 2D Materials. Small Methods, 2021, 5, 2101302.	4.6	4

#	Article	IF	CITATIONS
19	Quantum generative adversarial networks with multiple superconducting qubits. Npj Quantum Information, 2021, 7, .	2.8	14
20	Abnormal Spatial Shifts in Graphene Measured via the Beam Displacement Amplification Technique: Implications for Sensors Based on the Goos–Hächen Effect. ACS Applied Nano Materials, 2021, 4, 13477-13485.	2.4	2
21	Laser Writable Multifunctional van der Waals Heterostructures. Small, 2020, 16, e2003593.	5.2	13
22	Chemical vapor deposition of layered two-dimensional MoSi ₂ N ₄ materials. Science, 2020, 369, 670-674.	6.0	556
23	Superhigh Uniform Magnetic Cr Substitution in a 2D Mo 2 C Superconductor for a Macroscopicâ€5cale Kondo Effect. Advanced Materials, 2020, 32, 2002825.	11.1	7
24	Substrate effect on the photoluminescence of chemical vapor deposition transferred monolayer WSe2. Journal of Applied Physics, 2020, 128, 043101.	1.1	16
25	CdPS ₃ nanosheets-based membrane with high proton conductivity enabled by Cd vacancies. Science, 2020, 370, 596-600.	6.0	120
26	Back-Reflected Performance-Enhanced Flexible Perovskite Photodetectors through Substrate Texturing with Femtosecond Laser. ACS Applied Materials & Interfaces, 2020, 12, 26614-26623.	4.0	12
27	Photoresponse in a Strain-Induced Graphene Wrinkle Superlattice. Journal of Physical Chemistry Letters, 2020, 11, 5059-5067.	2.1	5
28	A gate-tunable symmetric bipolar junction transistor fabricated <i>via</i> femtosecond laser processing. Nanoscale Advances, 2020, 2, 1733-1740.	2.2	10
29	Fabrication, optical properties, and applications of twisted two-dimensional materials. Nanophotonics, 2020, 9, 1717-1742.	2.9	27
30	Transport through a network of two-dimensional NbC superconducting crystals connected via weak links. Physical Review B, 2020, 101, .	1.1	2
31	Tunneling devices based on graphene/black phosphorus van der Waals heterostructures. Materials Research Express, 2020, 7, 016310.	0.8	6
32	Second Time-Scale Synthesis of High-Quality Graphite Films by Quenching for Effective Electromagnetic Interference Shielding. ACS Nano, 2020, 14, 3121-3128.	7.3	57
33	Superhigh Electromagnetic Interference Shielding of Ultrathin Aligned Pristine Graphene Nanosheets Film. Advanced Materials, 2020, 32, e1907411.	11.1	310
34	Controllable Doping of Transitionâ€Metal Dichalcogenides by Organic Solvents. Advanced Electronic Materials, 2020, 6, 1901230.	2.6	10
35	A Flexible Carbon Nanotube Senâ€Memory Device. Advanced Materials, 2020, 32, e1907288.	11.1	48
36	Stacking of Exfoliated <scp>Twoâ€Dimensional</scp> Materials: A Review. Chinese Journal of Chemistry, 2020, 38, 981-995.	2.6	30

#	Article	IF	CITATIONS
37	High Yield Controlled Synthesis of Nano-Graphene Oxide by Water Electrolytic Oxidation of Glassy Carbon for Metal-Free Catalysis. ACS Nano, 2019, 13, 9482-9490.	7.3	25
38	Palladium nanoparticles supported on graphene acid: a stable and eco-friendly bifunctional C–C homo- and cross-coupling catalyst. Green Chemistry, 2019, 21, 5238-5247.	4.6	33
39	Ultrafast growth of nanocrystalline graphene films by quenching and grain-size-dependent strength and bandgap opening. Nature Communications, 2019, 10, 4854.	5.8	43
40	Interlayer epitaxy of wafer-scale high-quality uniform AB-stacked bilayer graphene films on liquid Pt3Si/solid Pt. Nature Communications, 2019, 10, 2809.	5.8	43
41	Dynamics of the passive synchronisation of erbium- and ytterbium-doped fibre Q-switched lasers with a common graphene saturable absorber. Laser Physics, 2019, 29, 085101.	0.6	4
42	Ultrafast nonlinear absorption and carrier relaxation in ReS2 and ReSe2 films. Journal of Applied Physics, 2019, 125, 173105.	1.1	17
43	Layer-Stacking, Defects, and Robust Superconductivity on the Mo-Terminated Surface of Ultrathin Mo ₂ C Flakes Grown by CVD. Nano Letters, 2019, 19, 3327-3335.	4.5	21
44	Ultrafast Transition of Nonuniform Graphene to High-Quality Uniform Monolayer Films on Liquid Cu. ACS Applied Materials & Interfaces, 2019, 11, 17629-17636.	4.0	10
45	Synergistic Effect of Aligned Graphene Nanosheets in Graphene Foam for Highâ€Performance Thermally Conductive Composites. Advanced Materials, 2019, 31, e1900199.	11.1	173
46	Optical properties of chemical vapor deposition-grown PtSe ₂ characterized by spectroscopic ellipsometry. 2D Materials, 2019, 6, 035011.	2.0	58
47	Anisotropic imaging for the highly efficient crystal orientation determination of two-dimensional materials. Journal of Materials Chemistry C, 2019, 7, 5945-5953.	2.7	7
48	Transport Properties of Topological Semimetal Tungsten Carbide in the 2D Limit. Advanced Electronic Materials, 2019, 5, 1800839.	2.6	5
49	Thickness-dependent ultrafast nonlinear absorption properties of PtSe2 films with both semiconducting and semimetallic phases. Applied Physics Letters, 2019, 115, .	1.5	21
50	Influence of sample depletion on Z-scan measurements of hydroxyl groups modified multi-walled carbon nanotubes dispersions. Materials Research Express, 2019, 6, 045611.	0.8	0
51	Fabrication of multiple nanopores in a SiNx membrane via controlled breakdown. Scientific Reports, 2018, 8, 1234.	1.6	33
52	Visualizing Photothermal Anisotropy in Black Phosphorus by Total Internal Reflection Pumpâ€Probe Technique. Advanced Materials Interfaces, 2018, 5, 1701605.	1.9	9
53	Preparation of high-quality graphene using triggered microwave reduction under an air atmosphere. Journal of Materials Chemistry C, 2018, 6, 1829-1835.	2.7	36
54	Blackâ€Phosphorusâ€Based Orientationâ€Induced Diodes. Advanced Materials, 2018, 30, 1704653.	11.1	53

#	Article	IF	CITATIONS
55	Carrier Engineering in Polarization-Sensitive Black Phosphorus van der Waals Junctions. ACS Applied Materials & Interfaces, 2018, 10, 35615-35622.	4.0	24
56	Polarizationâ€Dependent Photocurrent of Black Phosphorus/Rhenium Disulfide Heterojunctions. Advanced Materials Interfaces, 2018, 5, 1800960.	1.9	22
57	Muitilpe Nanopores Fabrication in a SiNX Membrane via Controlled Breakdown. Biophysical Journal, 2018, 114, 180a-181a.	0.2	0
58	Modulation of photothermal anisotropy using black phosphorus/rhenium diselenide heterostructures. Nanoscale, 2018, 10, 10844-10849.	2.8	18
59	High-accuracy measurement of the crystalline orientation of anisotropic two-dimensional materials using photothermal detection. Journal of Materials Chemistry C, 2018, 6, 5849-5856.	2.7	9
60	Photoinduced Orientationâ€Dependent Interlayer Carrier Transportation in Crossâ€Stacked Black Phosphorus van der Waals Junctions. Advanced Materials Interfaces, 2018, 5, 1800964.	1.9	8
61	Measuring third-order susceptibility tensor elements of monolayer MoS2 using the optical Kerr effect method. Applied Physics Letters, 2018, 113, 051901.	1.5	4
62	NiPS ₃ Nanosheet–Graphene Composites as Highly Efficient Electrocatalysts for Oxygen Evolution Reaction. ACS Nano, 2018, 12, 5297-5305.	7.3	104
63	Two-photon absorption and non-resonant electronic nonlinearities of layered semiconductor TlGaS ₂ . Optics Express, 2018, 26, 33895.	1.7	13
64	Tailoring the thermal and electrical transport properties of graphene films by grain size engineering. Nature Communications, 2017, 8, 14486.	5.8	154
65	Reduced graphene oxide-based optical sensor for detecting specific protein. Sensors and Actuators B: Chemical, 2017, 249, 142-148.	4.0	43
66	Phase transition and in situ construction of lateral heterostructure of 2D superconducting α/β Mo ₂ C with sharp interface by electron beam irradiation. Nanoscale, 2017, 9, 7501-7507.	2.8	28
67	Ultrafast Growth of Highâ€Quality Monolayer WSe ₂ on Au. Advanced Materials, 2017, 29, 1700990.	11.1	139
68	Strongly Coupled High-Quality Graphene/2D Superconducting Mo ₂ C Vertical Heterostructures with Aligned Orientation. ACS Nano, 2017, 11, 5906-5914.	7.3	110
69	Multiple-Nanopores Fabrication based on Dielectric Breakdown. Biophysical Journal, 2017, 112, 155a.	0.2	0
70	Phosphorene as a Polysulfide Immobilizer and Catalyst in Highâ€Performance Lithium–Sulfur Batteries. Advanced Materials, 2017, 29, 1602734.	11.1	289
71	Fast Growth and Broad Applications of 25â€Inch Uniform Graphene Glass. Advanced Materials, 2017, 29, 1603428.	11.1	90
72	Pulse width tunable passively Q-switched fiber laser with graphene saturable absorber. , 2017, , .		0

#	Article	IF	CITATIONS
73	Polarization dependence of graphene transient optical response: interplay between incident direction and anisotropic distribution of nonequilibrium carriers. Journal of the Optical Society of America B: Optical Physics, 2017, 34, 218.	0.9	6
74	Microshell Arrays Enhanced Sensitivity in Detection of Specific Antibody for Reduced Graphene Oxide Optical Sensor. Sensors, 2017, 17, 221.	2.1	5
75	Highâ€Precision Twistâ€Controlled Bilayer and Trilayer Graphene. Advanced Materials, 2016, 28, 2563-2570.	11.1	87
76	Scalable Clean Exfoliation of Highâ€Quality Few‣ayer Black Phosphorus for a Flexible Lithium Ion Battery. Advanced Materials, 2016, 28, 510-517.	11.1	336
77	Chemically modified graphene films for high-performance optical NO ₂ sensors. Analyst, The, 2016, 141, 4725-4732.	1.7	21
78	Magnetotransport Properties in High-Quality Ultrathin Two-Dimensional Superconducting Mo ₂ C Crystals. ACS Nano, 2016, 10, 4504-4510.	7.3	69
79	Optical Properties of Graphene and Its Applications under Total Internal Reflection. , 2016, , 687-700.		0
80	Photovoltage Enhancement in Twistedâ€Bilayer Graphene Using Surface Plasmon Resonance. Advanced Optical Materials, 2016, 4, 1703-1710.	3.6	29
81	Unique Domain Structure of Two-Dimensional α-Mo ₂ C Superconducting Crystals. Nano Letters, 2016, 16, 4243-4250.	4.5	101
82	Ultra-high sensitivity, multi-parameter monitoring of dynamical gas parameters using a reduced graphene oxide microcavity. Sensors and Actuators B: Chemical, 2016, 235, 474-480.	4.0	18
83	Broadband wavelength tunable mode-locked thulium-doped fiber laser operating in the 2 <i>μ</i> m region by using a graphene saturable absorber on microfiber. Laser Physics Letters, 2016, 13, 065105.	0.6	48
84	Reduced graphene oxide nanoshells for flexible and stretchable conductors. Nanotechnology, 2016, 27, 095301.	1.3	8
85	Reply to 'Do thermal effects cause the propulsion of bulk graphene material?'. Nature Photonics, 2016, 10, 139-141.	15.6	7
86	Investigation on a compact in-line multimode-single-mode-multimode fiber structure. Optics and Laser Technology, 2016, 80, 16-21.	2.2	50
87	Stable dual-wavelength laser combined with gain flattening ML-FMF Bragg grating filter. Optics Communications, 2016, 358, 1-5.	1.0	7
88	A general method for large-area and broadband enhancing photoresponsivity in graphene photodetectors. Applied Physics Letters, 2015, 107, .	1.5	15
89	Study on optical nonlinearity and optical limiting property of porphyrin-oxygenated carbon nanomaterial blends. Optoelectronics Letters, 2015, 11, 161-165.	0.4	2
90	All Optical Fiber Keyboard Based on 2D Location Sensor With Cascade Gratings. IEEE Photonics Technology Letters, 2015, 27, 1406-1409.	1.3	0

#	Article	IF	CITATIONS
91	1. Recent progresses on weak-light nonlinear optics. , 2015, , 1-104.		0
92	Switchable Dual-Wavelength SLM Fiber Laser Using Asymmetric PMFBG Fabry–Perot Cavities. IEEE Photonics Technology Letters, 2015, 27, 1281-1284.	1.3	9
93	Macroscopic and direct light propulsion of bulk graphene material. Nature Photonics, 2015, 9, 471-476.	15.6	192
94	Single-Frequency and Single-Polarization DFB Fiber Laser Based on Tapered FBG and Self-Injection Locking. IEEE Photonics Journal, 2015, 7, 1-9.	1.0	5
95	Stable single-polarization single-longitudinal-mode linear cavity erbium-doped fiber laser based on structured chirped fiber Bragg grating. Applied Optics, 2015, 54, 6.	0.9	14
96	Polarization dependence of optical pump-induced change of graphene extinction coefficient. Optical Materials Express, 2015, 5, 1550.	1.6	14
97	Actively Q-switched ytterbium-doped fiber laser by an all-optical Q-switcher based on graphene saturable absorber. Optics Express, 2015, 23, 21490.	1.7	18
98	Making transient optical reflection of graphene polarization dependent. Optics Express, 2015, 23, 24177.	1.7	5
99	Sign of differential reflection and transmission in pump-probe spectroscopy of graphene on dielectric substrate. Photonics Research, 2015, 3, A1.	3.4	12
100	Large-area synthesis of high-quality and uniform monolayer WS2 on reusable Au foils. Nature Communications, 2015, 6, 8569.	5.8	336
101	Large-area high-quality 2D ultrathin Mo2C superconducting crystals. Nature Materials, 2015, 14, 1135-1141.	13.3	1,045
102	Characteristics of a high extinction ratio comb-filter based on LP01–LP11even mode elliptical multilayer-core fibers. Optical Fiber Technology, 2015, 21, 103-109.	1.4	10
103	Nonlinear optical and optical limiting properties of fullerene, multi-walled carbon nanotubes, graphene and their derivatives with oxygen-containing functional groups. Journal of Optics (United) Tj ETQq1 1 ().7 &⊕ 314	rg&&/Overlo
104	Synthesis, Characterization and Photophysical Properties of Graphene-Phthalocyanine Hybrid. Asian Journal of Chemistry, 2014, 26, 4819-4826.	0.1	1
105	Experimental observation of a giant Goos–HÃ ¤ chen shift in graphene using a beam splitter scanning method. Optics Letters, 2014, 39, 5574.	1.7	81
106	Tunable and switchable dual-wavelength single polarization narrow linewidth SLM erbium-doped fiber laser based on a PM-CMFBG filter. Optics Express, 2014, 22, 22528.	1.7	53
107	Flexible graphene saturable absorber on two-layer structure for tunable mode-locked soliton fiber laser. Optics Express, 2014, 22, 10239.	1.7	33
108	Evolution of anisotropic-to-isotropic photoexcited carrier distribution in graphene. Physical Review B. 2014, 90	1.1	20

#	Article	IF	CITATIONS
109	Characteristics of HE ₁₁ -HE ₂₁ mode elliptical multilayer-core fiber with low nonlinearity. Optical Engineering, 2014, 53, 105104.	0.5	4
110	Ultrasensitive Flow Sensing of a Single Cell Using Graphene-Based Optical Sensors. Nano Letters, 2014, 14, 3563-3569.	4.5	116
111	Temperature-Independent and Strain-Independent Twist Sensor Based on Structured PM-CFBG. IEEE Photonics Technology Letters, 2014, 26, 1565-1568.	1.3	28
112	Large tunable optical absorption of CVD graphene under total internal reflection by strain engineering. Nanotechnology, 2014, 25, 455707.	1.3	8
113	Photocatalysis: Constructing a Metallic/Semiconducting TaB2/Ta2O5Core/Shell Heterostructure for Photocatalytic Hydrogen Evolution (Adv. Energy Mater. 12/2014). Advanced Energy Materials, 2014, 4, n/a-n/a.	10.2	0
114	Pulse-Width Tuning in a Passively Mode-Locked Fiber Laser With Graphene Saturable Absorber. IEEE Photonics Technology Letters, 2014, 26, 360-363.	1.3	11
115	Tunable graphene saturable absorber with cross absorption modulation for mode-locking in fiber laser. Applied Physics Letters, 2014, 105, .	1.5	38
116	Constructing a Metallic/Semiconducting TaB ₂ /Ta ₂ O ₅ Core/Shell Heterostructure for Photocatalytic Hydrogen Evolution. Advanced Energy Materials, 2014, 4, 1400057.	10.2	44
117	Linear and Nonlinear Optical Properties ofmeso-Tetra(4-ferrocenylcarbonyloxyphenyl)porphyrin and Its Zinc(â¡) Complex. Chinese Journal of Organic Chemistry, 2014, 34, 371.	0.6	0
118	Broadband all-optical modulation using a graphene-covered-microfiber. Laser Physics Letters, 2013, 10, 065901.	0.6	86
119	Saturable Absorber Based on Graphene-Covered-Microfiber. IEEE Photonics Technology Letters, 2013, 25, 1392-1394.	1.3	35
120	Nonlinear optical and optical limiting properties of graphene hybrids covalently functionalized by phthalocyanine. Chemical Physics Letters, 2013, 577, 62-67.	1.2	51
121	Increased optical nonlinearities of multi-walled carbon nanotubes covalently functionalized with porphyrin. Carbon, 2013, 51, 419-426.	5.4	38
122	Accurate layers determination of graphene on transparent substrate based on polarization-sensitive absorption effect. Applied Physics Letters, 2013, 103, .	1.5	17
123	Bulk functionalization of graphene using diazonium compounds and amide reaction. Applied Surface Science, 2013, 280, 914-919.	3.1	28
124	High-quality and efficient transfer of large-area graphene films onto different substrates. Carbon, 2013, 56, 271-278.	5.4	143
125	Polarization-dependent optical absorption of graphene under total internal reflection. Applied Physics Letters, 2013, 102, .	1.5	95
126	Solution-processable graphene mesh transparent electrodes for organic solar cells. Nano Research, 2013. 6. 478-484.	5.8	53

#	Article	IF	CITATIONS
127	Transparent and flexible multi-layer films with graphene recording layers for optical data storage. Applied Physics Letters, 2013, 102, .	1.5	16
128	Enhanced reverse saturable absorption and optical limiting properties in a protonated water-soluble porphyrin. Journal of Optics (United Kingdom), 2013, 15, 055206.	1.0	12
129	The selective transfer of patterned graphene. Scientific Reports, 2013, 3, 3216.	1.6	21
130	Actively manipulation of operation states in passively pulsed fiber lasers by using graphene saturable absorber on microfiber. Optics Express, 2013, 21, 14859.	1.7	44
131	Transient thermal effect, nonlinear refraction and nonlinear absorption properties of graphene oxide sheets in dispersion. Optics Express, 2013, 21, 7511.	1.7	99
132	Optical limiting effect and ultrafast saturable absorption in a solid PMMA composite containing porphyrin-covalently functionalized multi-walled carbon nanotubes. Optics Express, 2013, 21, 25277.	1.7	26
133	Evanescent-wave photoacoustic spectroscopy with optical micro/nano fibers. Optics Letters, 2012, 37, 214.	1.7	52
134	Polarization characteristics of nonlinear refraction and nonlinear scattering in several solvents. Journal of the Optical Society of America B: Optical Physics, 2012, 29, 2721.	0.9	6
135	Wavelength-tunable, passively mode-locked fiber laser based on graphene and chirped fiber Bragg grating. Optics Letters, 2012, 37, 2394.	1.7	95
136	Sensitive Real-Time Monitoring of Refractive Indexes Using a Novel Graphene-Based Optical Sensor. Scientific Reports, 2012, 2, 908.	1.6	72
137	Synthesis, Photophysical and Electrochemical Properties of Amideâ€Linked Phthalocyanineâ€Fullerene Dyad. Chinese Journal of Chemistry, 2012, 30, 1766-1770.	2.6	7
138	Nonlinear optical properties of graphene-based materials. Science Bulletin, 2012, 57, 2971-2982.	1.7	144
139	Effects of solvent on nonlinear absorption properties of tetraphenylporphyrin compounds in the nanosecond regime. Optik, 2012, 123, 1015-1018.	1.4	2
140	Passively Mode-Locked Fiber Laser Based on Reduced Graphene Oxide on Microfiber for Ultra-Wide-Band Doublet Pulse Generation. Journal of Lightwave Technology, 2012, 30, 984-989.	2.7	67
141	Direct patterning on reduced graphene oxide nanosheets using femtosecond laser pulses. Journal of Optics (United Kingdom), 2011, 13, 085601.	1.0	18
142	Ultrafast carrier dynamics and saturable absorption of solution-processable few-layered graphene oxide. Applied Physics Letters, 2011, 98, .	1.5	143
143	Ultrafast Dynamics and Nonlinear Optical Responses from sp ² - and sp ³ -Hybridized Domains in Graphene Oxide. Journal of Physical Chemistry Letters, 2011, 2, 1972-1977.	2.1	166
144	Nonlinear optical and optical limiting properties of graphene oxide–Fe ₃ O ₄ hybrid material. Journal of Optics (United Kingdom), 2011, 13, 075202.	1.0	93

#	Article	IF	CITATIONS
145	Third-order nonlinear susceptibility tensor elements of CS_2 at femtosecond time scale. Optics Express, 2011, 19, 5559.	1.7	32
146	Discriminating thermal effect in nonlinear-ellipse-rotation-modified Z-scan measurements. Optics Letters, 2011, 36, 2086.	1.7	14
147	Passively mode-locked fiber laser based on a hollow-core photonic crystal fiber filled with few-layered graphene oxide solution. Optics Letters, 2011, 36, 3024.	1.7	146
148	Study on Z-scan characteristics of multilayer nonlinear media using coordinate transformation method. Optik, 2010, 121, 2172-2175.	1.4	0
149	Nonlinear optical properties of hydroxyl groups modified multi-walled carbon nanotubes. Chemical Physics Letters, 2010, 494, 75-79.	1.2	16
150	Toward All-Carbon Electronics: Fabrication of Graphene-Based Flexible Electronic Circuits and Memory Cards Using Maskless Laser Direct Writing. ACS Applied Materials & Interfaces, 2010, 2, 3310-3317.	4.0	55
151	Modified elliptically polarized light Z-scan method for studying third-order nonlinear susceptibility components. Optics Express, 2010, 18, 10270.	1.7	5
152	Analysis on the origin of the ultrafast optical nonlinearity of carbon disulfide around 800 nm. Optics Express, 2010, 18, 26169.	1.7	15
153	Synthesis, Characterization and Nonlinear Optical Property of Graphene-C ₆₀ Hybrid. Journal of Nanoscience and Nanotechnology, 2009, 9, 5752-5756.	0.9	29
154	A Graphene Hybrid Material Covalently Functionalized with Porphyrin: Synthesis and Optical Limiting Property. Advanced Materials, 2009, 21, 1275-1279.	11.1	1,007
155	Photoconductivity of Bulkâ€Filmâ€Based Graphene Sheets. Small, 2009, 5, 1682-1687.	5.2	80
156	Synthesis, characterization and optical limiting property of covalently oligothiophene-functionalized graphene material. Carbon, 2009, 47, 3113-3121.	5.4	218
157	<i>In situ</i> synthesis and third-order nonlinear optical properties of CdS/PVP nanocomposite films. Journal Physics D: Applied Physics, 2009, 42, 075402.	1.3	23
158	Polarization dependence of Z-scan measurement: theory and experiment. Optics Express, 2009, 17, 6397.	1.7	35
159	Enhanced nonlinear optical properties of graphene-oligothiophene hybrid material. Optics Express, 2009, 17, 23959.	1.7	57
160	Porphyrin and Fullerene Covalently Functionalized Graphene Hybrid Materials with Large Nonlinear Optical Properties. Journal of Physical Chemistry B, 2009, 113, 9681-9686.	1.2	435
161	Nonlinear optical properties of graphene oxide in nanosecond and picosecond regimes. Applied Physics Letters, 2009, 94, .	1.5	304
162	Enhanced Optical Limiting Effects in Porphyrinâ€Covalently Functionalized Singleâ€Walled Carbon Nanotubes. Advanced Materials, 2008, 20, 511-515.	11.1	164

#	Article	IF	CITATIONS
163	Effects of metallization and bromination on nonlinear optical properties of diphenylporphyrins. Optics Communications, 2008, 281, 776-781.	1.0	14
164	Evolutions of polarization and nonlinearities in an isotropic nonlinear medium. Optics Express, 2008, 16, 8144.	1.7	8
165	Study on optical nonlinearities of porphyrin covalently functionalized single-wall carbon nanotubes. , 2008, , .		3
166	Nonlinear absorption and optical limiting properties of carbon disulfide in a short-wavelength region. Journal of the Optical Society of America B: Optical Physics, 2007, 24, 1101.	0.9	22
167	Nonlinear ellipse rotation modified Z-scan measurements of third-order nonlinear susceptibility tensor. Optics Express, 2007, 15, 13351.	1.7	24
168	Study on Nonlinear Spectroscopy of Tetraphenylporphyrin and Dithiaporphyrin Diacids. Journal of Physical Chemistry B, 2007, 111, 14136-14142.	1.2	32
169	Synthesis and crystal structure of 21,23-dithiaporphyrins and their nonlinear optical activities. Tetrahedron Letters, 2007, 48, 5687-5691.	0.7	13
170	Method for measurements of second-order nonlinear optical coefficient based on Z-scan. Optics Communications, 2007, 274, 213-217.	1.0	5
171	Covalently porphyrin-functionalized single-walled carbon nanotubes: a novel photoactive and optical limiting donor–acceptor nanohybrid. Journal of Materials Chemistry, 2006, 16, 3021-3030.	6.7	211
172	Nonlinear Absorption and Nonlinear Refraction of Self-Assembled Porphyrins. Journal of Physical Chemistry B, 2006, 110, 15140-15145.	1.2	23
173	Effect of groove periodicity on the enhanced transmission through a single subwavelength slit. Journal of the Optical Society of America B: Optical Physics, 2006, 23, 1517.	0.9	0
174	Active tuning of nonlinear absorption in a supramolecular zinc diphenylporphyrin-pyridine system. Optics Express, 2006, 14, 2770.	1.7	4
175	Characteristics of co-existence of third-order and transient thermally induced optical nonlinearities in nanosecond regime. Optics Communications, 2005, 245, 377-382.	1.0	9
176	Coordinate transformation and coordinate mapping for numerical simulation of Z-scan measurements. Optics Communications, 2005, 244, 71-77.	1.0	3
177	Modified local one-dimensional beam-propagation method based on the Douglas scheme. Optics Communications, 2005, 256, 210-215.	1.0	0
178	Study on Z-scan characteristics for a large nonlinear phase shift. Journal of the Optical Society of America B: Optical Physics, 2005, 22, 1911.	0.9	49
179	Enhanced light transmission through a single subwavelength aperture in layered films consisting of metal and dielectric. Optics Express, 2005, 13, 9071.	1.7	32
180	Analysis of Z-scan of thick media with nonlinear refraction and absorption for elliptic Gaussian beam by variational approach. Optics Communications, 2004, 237, 221-227.	1.0	8

#	Article	IF	CITATIONS
181	Analytic solutions to Z-scan characteristics of thick media with nonlinear refraction and nonlinear absorption. Journal of the Optical Society of America B: Optical Physics, 2004, 21, 63.	0.9	27
182	Accurate determination of nonlinear refraction and nonlinear absorption by a single Z-scan method. Journal of the Optical Society of America B: Optical Physics, 2004, 21, 349.	0.9	15
183	Local one-dimensional approximation for fast simulation of Z-scan measurements with an arbitrary beam. Applied Optics, 2004, 43, 4408.	2.1	14
184	Flexible alteration of optical nonlinearities of iodine charge-transfer complexes in solutions. Optics Letters, 2004, 29, 1099.	1.7	23
185	Analysis of Z-scan of thick media with high-order nonlinearity by variational approach. Optics Communications, 2003, 219, 411-419.	1.0	22
186	Variational analysis of z scan of thick medium with an elliptic Gaussian beam. Applied Optics, 2003, 42, 2219.	2.1	14
187	Large optical nonlinearities of new organophosphorus fullerene derivatives. Applied Optics, 2003, 42, 7072.	2.1	11
188	Comparison of the solutions from a novel variational method with numerical results for the study of beam propagation in a Kerr medium with nonlinear absorption. Optics Letters, 2003, 28, 722.	1.7	6
189	In-fiber liquid-level probe based on Michelson interferometer via dual-mode elliptical multilayer-core fiber. Journal of Modern Optics, 0, , 1-6.	0.6	11
190	Resonant Scattering in Proximity oupled Graphene/Superconducting Mo ₂ C Heterostructures. Advanced Science, 0, , 2201343.	5.6	1